

Weibel Instability Driven by Relativistic Pair Jets: Particle Acceleration, Magnetic Field Generation, and Emission

K.-I. Nishikawa

National Space Science and Technology Center, Huntsville, AL 35805 USA

P. Hardee

Department of Physics and Astronomy, University of Alabama, Tuscaloosa, AL 35487 USA

C. B. Hededal

*Niels Bohr Institute, Department of Astrophysics,
Juliane Maries Vej 30, 2100 København Ø, Denmark*

G. Richardson

Department of Mechanical and Aerospace Engineering University of Alabama in Huntsville, AL 35899 USA

H. Sol

LUTH, Observatoire de Paris-Meudon, 5 place Jules Jansen 92195 Meudon Cedex, France

R. Preece

*Department of Physics, University of Alabama in Huntsville,
AL 35899 and National Space Science and Technology Center, Huntsville, AL 35805 USA*

G. J. Fishman

*NASA-Marshall Space Flight Center,
National Space Science and Technology Center,
Huntsville, AL 35805 USA*

Shock acceleration is a ubiquitous phenomenon in astrophysical plasmas. Plasma waves and their associated instabilities (e.g., Buneman, Weibel and other two-stream instabilities) created in collisionless shocks are responsible for particle (electron, positron, and ion) acceleration. Using a 3-D relativistic electromagnetic particle (REMP) code, we have investigated particle acceleration associated with a relativistic jet front propagating into an ambient plasma. We find that the growth times of the Weibel instability in electron-positron jets are not affected by the (electron-positron or electron-ion) ambient plasmas. However, the amplitudes of generated local magnetic fields in the electron-ion ambient plasma are significantly larger than those in the electron-positron ambient plasma. The small scale magnetic field structure generated by the Weibel instability is appropriate to the generation of “jitter” radiation from deflected electrons (positrons) as opposed to synchrotron radiation. The jitter radiation resulting from small angle deflected electrons may be important for understanding the complex time structure and spectral evolution observed in gamma-ray bursts and other astrophysical sources containing relativistic jets and relativistic collisionless shocks.

I. INTRODUCTION

Nonthermal radiation observed from astrophysical systems containing relativistic jets and shocks, e.g., active galactic nuclei (AGNs), gamma-ray bursts (GRBs), and Galactic microquasar systems usually has power-law emission spectra. In most of these systems, the emission is thought to be generated by accelerated electrons through the synchrotron and/or inverse Compton mechanisms. Radiation from these systems is observed in the radio through the gamma-ray region. Radiation in optical and higher frequencies typically requires particle re-acceleration in order to counter radiative losses.

Fermi acceleration is the mechanism usually assumed for the acceleration of particles in astrophysical

environments characterized by a power-law spectrum. This mechanism for particle acceleration relies on the shock jump conditions in relativistic shocks [e.g., 1, 2]. Most astrophysical shocks are collisionless since dissipation is dominated by wave-particle interactions rather than particle-particle collisions. Diffusive shock acceleration (DSA) relies on repeated scattering of charged particles by magnetic irregularities (Alfvén waves) to confine the particles near the shocks. However, particle acceleration near relativistic shocks cannot be characterized as DSA because the propagation of accelerated particles ahead of the shock cannot be described by spatial diffusion. Anisotropies in the angular distribution of the accelerated particles are large, and the diffusion approximation for spatial transport does not apply [3].

Particle-in-cell (PIC) simulations can shed light on

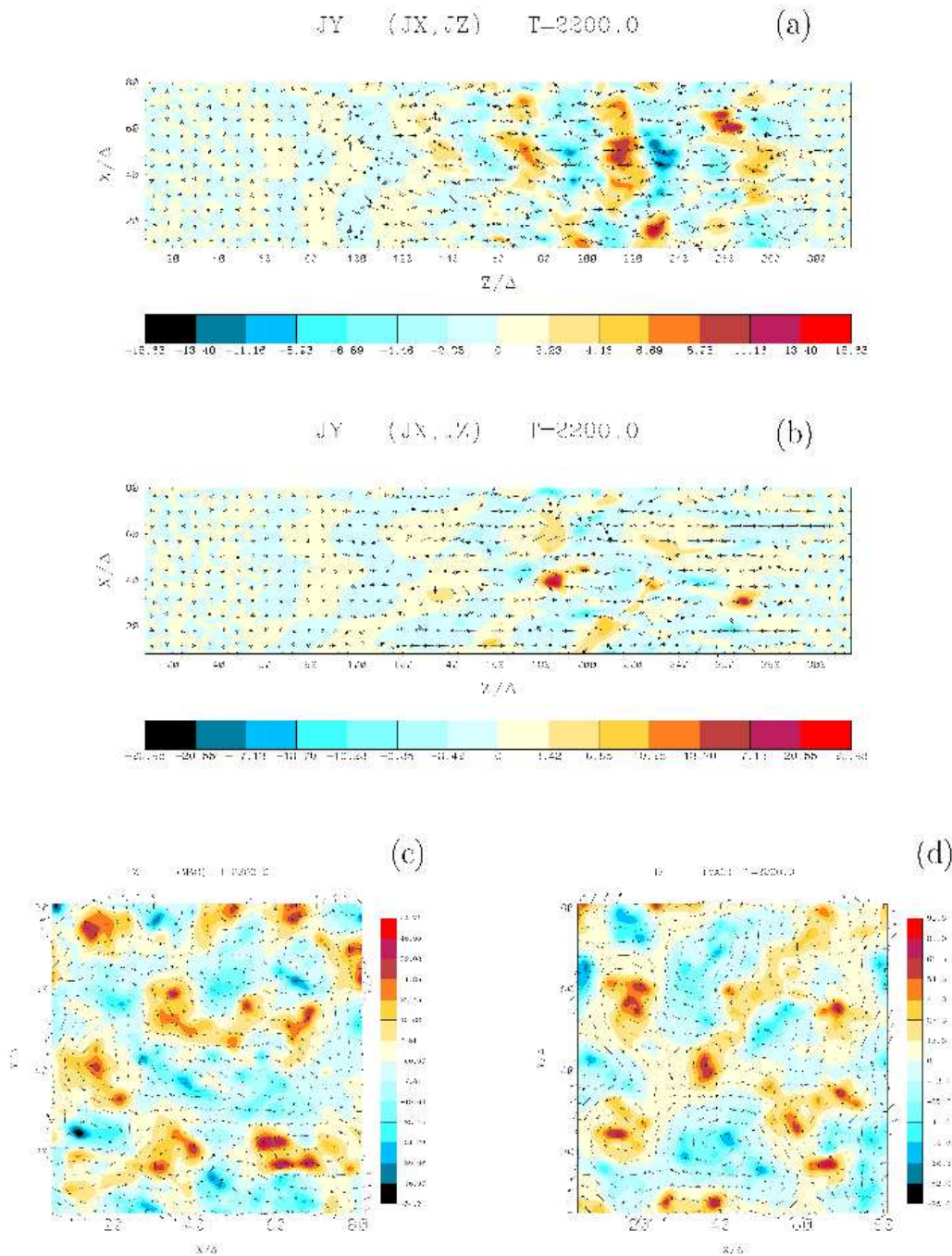


FIG. 1: 2D images in the $x-z$ plane at $y = 43\Delta$ ((a) and (b)) and in the $x-y$ plane at $z = 230\Delta$ a flat jet injected into a unmagnetized ambient medium shown at $t = 28.8/\omega_{pe}$. Colors indicate the y -component of the current density (J_y) ((a) and (b)) and z -component of the current density (J_z) ((c) and (d)) for electron-positron ((a) and (c)) and electron-ion ((b) and (d)) ambient plasmas. Their peaks are (a) 15.6, (b) 23.9, (c) 54.7, and (d) 95.6. Arrows show J_z, J_x ((a) and (b)) and B_x, B_y ((c) and (d)).

the physical mechanism of particle acceleration that occurs in the complicated dynamics within relativistic shocks. Recent PIC simulations using injected relativistic electron-ion jets show that acceleration occurs within the downstream jet, rather than by the scat-

tering of particles back and forth across the shock as in Fermi acceleration [4-10]. In general, these independent simulations have confirmed that relativistic jets excite the Weibel instability [11]. The Weibel instability generates current filaments with associated

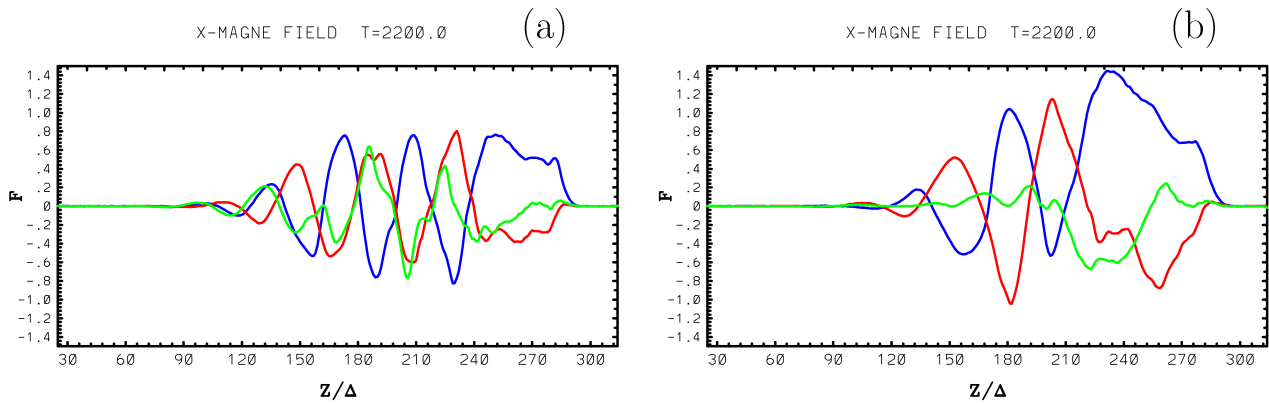


FIG. 2: One-dimensional cuts along the z -direction ($25 \leq z/\Delta \leq 154$) of a flat jet. Shown are the x -components of the magnetic field shown at $t = 238.8/\omega_{pe}$ for unmagnetized electron-positron (a) and electron-ion (b) ambient plasmas. Cuts are taken at $x/\Delta = 38$ and $y/\Delta = 33$ (blue), 43(red), 53(green) and separated by about an electron skin depth.

magnetic fields [12], and accelerates electrons [4-10].

In this paper we present new simulation results of particle acceleration and magnetic field generation in relativistic electron-positron shocks using 3-D relativistic electromagnetic particle-in-cell (REMP) simulations. We have performed two simulations in which an electro-positron jet is injected into two different ambient plasmas (electron-positron and electron-ion). In our new simulations, the growth rate of the Weibel instability and its evolution with different ambient plasmas have been studied without an initial ambient magnetic field.

II. SIMULATION SETUP AND RESULTS

Two simulations were performed using an $85 \times 85 \times 320$ grid with a total of 180 million particles (27 particles/cell/species for the ambient plasma) and an electron skin depth, $\lambda_{ce} = c/\omega_{pe} = 9.6\Delta$, where $\omega_{pe} = (4\pi e^2 n_e/m_e)^{1/2}$ is the electron plasma frequency and Δ is the grid size [5, 8].

The particle number density of the jet is $0.741n_b$, where n_b is the density of ambient (background) electrons. The average jet velocities in the two simulations are $v_j = 0.9798c$ corresponding to Lorentz factors of 5 (2.0 MeV). The jets are cold ($v_{j,th}^e = v_{j,th}^p = 0.01c$) in the rest frame of the ambient plasma where c is the speed of light. Electron-positron plasmas have mass ratio $m_p/m_e = 1$. The mass ratio of ion and electron is $m_i/m_e = 20$. The electron (positron) and ion thermal velocities in the ambient plasmas are $v_{th}^e = v_{th}^p = 0.1c$ and $v_{th}^i = 0.022c$, respectively. The time step $\Delta t = 0.013/\omega_{pe}$.

The electrons are deflected by the transverse magnetic fields (B_x, B_y) via the Lorentz force: $-e(\mathbf{v} \times \mathbf{B})$, generated by current filaments (J_z), which in turn en-

hance the transverse magnetic fields [5, 6, 8]. The complicated filamented structures resulting from the Weibel instability have diameters on the order of the electron skin depth ($\lambda_{ce} = 9.6\Delta$). This is in good agreement with the prediction of $\lambda \approx 2^{1/4} c \gamma_{th}^{1/2} / \omega_{pe} \approx 1.188 \lambda_{ce} = 11.4\Delta$ [12]. Here, $\gamma_{th} \sim 1$ is a thermal Lorentz factor. At the earlier time smaller current filaments are generated. However, in the electron-positron jets because of larger growth rates, the current filaments are coalesced in the transverse direction in the nonlinear stage as shown by Nishikawa et al. [13, 14]. The longitudinal current (J_z) in the electron-positron jet shows significantly more transverse variation than in the electron-ion jets [13, 14].

Current filaments resulting from development of the Weibel instability behind the jet front are shown in Fig. 1 at time $t = 28.8/\omega_{pe}$ for unmagnetized electron-positron ((a) and (c)) and electron-ion ((b) and (d)) ambient plasmas. Figures 1a and 1b show the y -component of the current density in the $z-x$ plane at $y = 43\Delta$. The maximum values of J_y are (a) 15.6 and (b) 23.9, respectively. The arrows show the perturbed currents (J_z, J_x). Figures 1c and 1d show the z -component of the current density in the $x-y$ plane at $z = 230\Delta$. The arrows show the magnetic fields (B_x, B_y) created by J_z and their maximum values are (c) 54.7 and (d) 95.6, respectively. Based on these figures the maximum values of the generated current densities (magnetic fields) are larger in the electron-ion ambient plasmas. The ambient ions are responsible for the larger maximum current densities.

It should be noted that as shown in the previous work for the different jet types ((a) electron-positron and (b) electron-ion) injected into ambient plasmas with the jet composition, the maximum current densities have different structures [13, 14]. Current filaments resulting from development of the Weibel

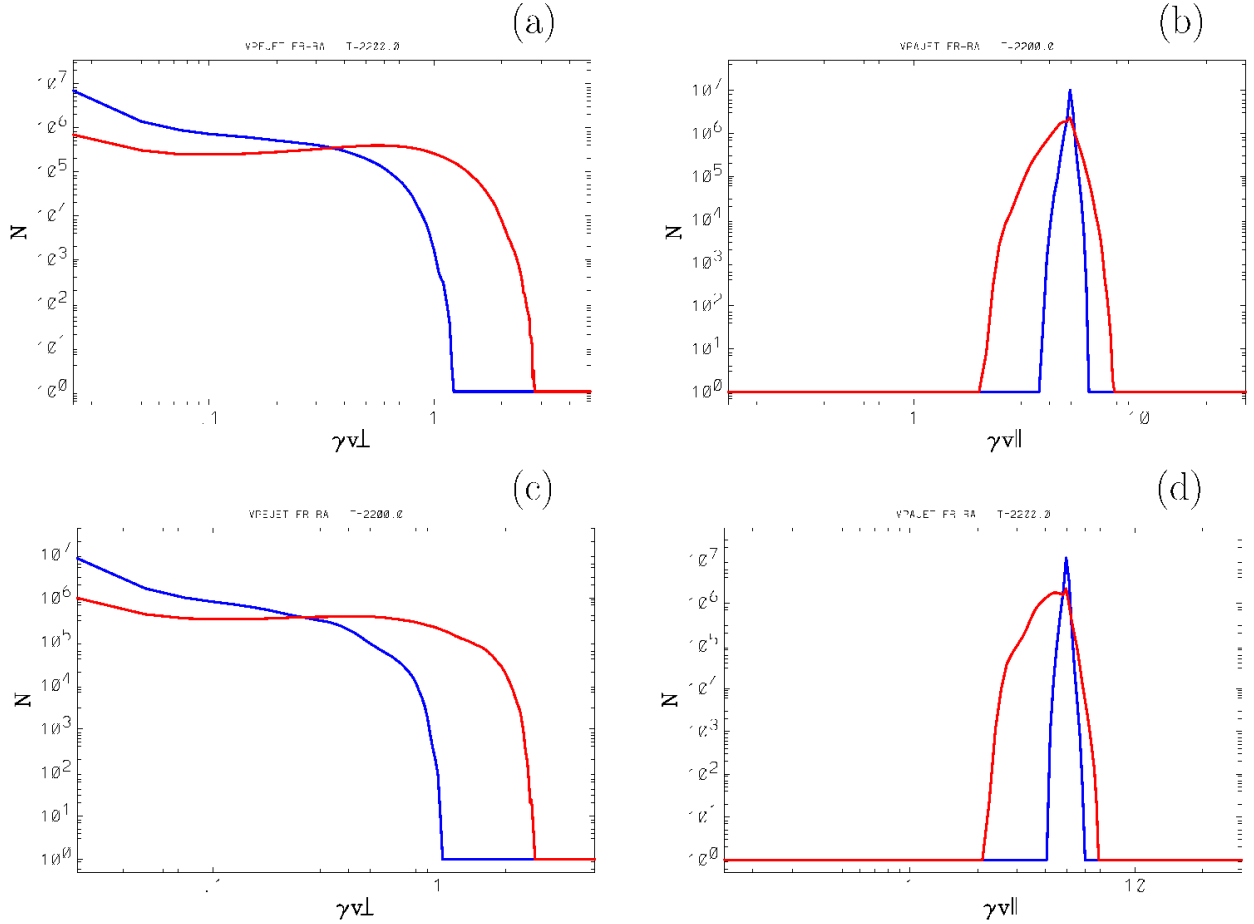


FIG. 3: Velocity distributions of jet electrons two cases as Fig. 1 at $t = 28.8/\omega_{pe}$ ((a) and (b): electron-positron ambient plasma, (c) and (d) electron-ion ambient plasma. Jet electrons are binned as a function of γv_{\perp} ((a) and (c)) and γv_{\parallel} ((b) and (d)), and γv_{\perp} , where $\gamma = (1 - (v_{\parallel}^2 + v_{\perp}^2)/c^2)^{-1/2}$. The blue and red curves show the distributions of injected and shocked jet electrons.

instability behind the jet front (at $z = 230\Delta$) are obtained at time $t = 28.8/\omega_{pe}$ for two different cases with unmagnetized ambient plasmas. The maximum values of J_z are (a) ± 54.7 (as same as Fig. 1a), (b) -123.6 , respectively. The electron-positron jets show electron (negative) and positron (positive) current filamentations, since both species contribute to the Weibel instability. On the other hand, at this simulation time mainly electron jets generate (negative) current filamentations. In the electron-ion jet at this time only electrons are contributing in exciting the Weibel instability, electron current channels are dominate, therefore J_z has the negative value.

The differences in the generated current densities (J_z) between the different ambient plasmas are seen more clearly in the x -component of the generated magnetic fields as shown in Fig. 2. The amplitudes of B_x in the electron-ion ambient plasma (b) are much larger than those in the electron-positron

ambient plasma (a). The distances between peaks in (b) are clearly larger than those in (a). This seems to come from the fact that the ambient ions are affecting the growth of the Weibel instability. These differences in the amplitudes and structures will affect the emission, which needs to be calculated from an ensemble of all particles (electrons and positrons). Since magnetic fields are generated by the Weibel instability “jitter” radiation need to be considered by the deflected electrons (positrons) [15, 16, 17]. In order to examine the saturated magnetic fields we need much longer simulations, which are in progress at the present time.

The Weibel instability is aperiodic, i.e., $\omega_{\text{real}} \sim 0$ (convective) [12]. Thus, it can be saturated only by nonlinear effects and not by kinetic effects, such as collisionless damping or resonance broadening. Hence the magnetic field can be amplified to very high values. This characteristic is seen in Fig. 2b. The time

evolution of the B_x shows that its amplitudes grow as the jet propagates without any significant oscillations in the frame of the jet.

Simulation results show that smaller scale current filaments appear immediately behind the jet front. Smaller filaments merge into larger filaments behind the jet front in the non-linear stage. This phenomenon is seen in Fig. 2. In particular Figure 2b shows a large and long wavelength just behind the jet front.

It should be noted that a long simulation with electron-ion jet with $\gamma = 15$ show that the electron Weibel instability switches to the ion Weibel instability [9]. The ion current channels with the ion skin depth contribute to accelerating electrons [4, 7, 9].

The acceleration of electrons has been reported in previous work [4-10, 13, 14]. Figure 3 shows that the cold jet electrons are accelerated and decelerated. As expected, at this time jet electrons in the electron-positron ambient plasma (b) are thermalized more strongly than those in the electron-ion ambient plasma (d). The blue curves in Figs. 3b and 3d are close to the initial distribution of injected jet electrons (half of jet electrons). We also see that the kinetic energy (parallel velocity $v_{\parallel} \approx v_j$) of the jet electrons is transferred to the perpendicular velocity via the electric and magnetic fields generated by the Weibel instability [11, 12]. The strongest transverse acceleration of jet electrons accompanies the strongest deceleration of electron flow and occurs between $z/\Delta = 210 - 240$. The transverse velocity distribution of jet in the electron-positron ambient plasma (at the peak value) is slightly more accelerated than that in the electron-ion ambient plasma as shown in the red curves in Figs. 3a and 3c. The strongest acceleration takes place around the maximum amplitude of perturbations due to the Weibel instability at $z/\Delta \sim 230$ as seen in Figs 1a and 1b.

III. SUMMARY AND DISCUSSION

We have performed self-consistent, three-dimensional relativistic particle simulations of relativistic electron-positron jets propagating into unmagnetized electron-positron and electron-ion ambient plasmas. The main acceleration of electrons takes place in the region behind the shock front [4-5, 7-10, 13, 14, 17]. Processes in the relativistic collisionless shock are dominated by structures produced by the Weibel instability. This instability is excited in the downstream region behind the jet head, where electron density perturbations lead to the formation of current filaments. The nonuniform electric field and magnetic field structures associated with these current filaments decelerate the jet electrons and positrons, while accelerating the ambient electrons and positrons, and accelerating (heating) the jet and ambient electrons and positrons in the transverse

direction.

The effects of the different ambient plasmas have been investigated in this report. In spite of the local larger current filaments generated in the electron-ion ambient plasma, the total jet electron acceleration is smaller than that in the electron-positron ambient plasma.

The growth rates depend on the Lorentz factors of the jet as suggested by the theory [12]. E -fold time is written as $\tau \simeq \sqrt{\gamma_{\text{sh}}}/\omega_{\text{pe}}$, where γ_{sh} is the Lorentz factor of the shock. The simulation results show that the growth time becomes larger with the larger Lorentz factor [18].

Other simulations with different skin depths and plasma frequencies confirm that both simulations have enough resolution and the electron Weibel instability is characterized by the electron skin depth [8].

An additional simulation in which an electron-ion jet is injected into an ambient plasma with perpendicular magnetic field shows magnetic reconnection due to the generation of an antiparallel magnetic field generated by bending of jet electron trajectories, consequently jet electrons are subject to strong non-thermal acceleration [10].

The generation of magnetic fields both with and without an initial magnetic field suggests that emission in GRB afterglows and Crab-like pulsar winds could be either synchrotron or jitter emission [15, 16, 17]. The filament sizes appear to be smaller than can produce observable variations in intensity structure. However, this small size can mean that the deflection angle, $\alpha \sim eB_{\perp}\lambda_B/\gamma m_e c^2$, of particles by Weibel filaments is smaller than the radiation beaming angle, $\Delta\theta \sim 1/\gamma$ [12]. Here $\lambda_B \sim \lambda_{ce}$, $eB_{\perp}/m_e c < \Omega_e$, and the ratio $\delta \sim \alpha/\Delta\theta < \Omega_e/\omega_{\text{pe}}$ will be less than one when the cyclotron frequency is less than the plasma frequency. Thus, when ambient magnetic fields are moderate, i.e., the cyclotron frequency is less than the plasma frequency and $\delta < 1$, the emission may correspond to jitter rather than synchrotron radiation [15, 16, 17].

The fundamental characteristics of relativistic shocks are essential for a proper understanding of the prompt gamma-ray and afterglow emission in gamma-ray bursts, and also to an understanding of the particle reacceleration processes and emission from the shocked regions in relativistic AGN jets. Since the shock dynamics is complex and subtle, more comprehensive studies are required to better understand the acceleration of electrons, the generation of magnetic fields and the associated emission. This further study will provide insight into basic relativistic collisionless shock characteristics needed to provide a firm physical basis for modeling the emission from shocks in relativistic flows.

Acknowledgments

K. Nishikawa is a NRC Senior Research Fellow at NASA Marshall Space Flight Center. This research (K.N.) is partially supported by the National Science Foundation awards ATM-0100997, and INT-9981508. P. Hardee acknowledges partial support by a Na-

tional Space Science and Technology (NSSTC/NASA) award. The simulations have been performed on IBM p690 at the National Center for Supercomputing Applications (NCSA) which is supported by the National Science Foundation.

-
- [1] Y. A. Gallant, Particle Acceleration at Relativistic Shocks, in *Relativistic Flows in Astrophysics*, eds. A. W. Guthmann, M. Georganopoulos, A. Marcowith, & K. Manolokou, Lecture Notes in Physics, Springer Verlag, (2002) astro-ph/0201243
- [2] J. Niemiec and M. Ostrowski, M., Cosmic-Ray Acceleration at Relativistic Shock Waves with A Relativistic Magnetic Field Structure, *ApJ*, **610**, 851 (2004)
- [3] A. Achterberg, Y. A. Gallant, J. G. Kirk, and A. X. Guthmann, Particle acceleration by ultrarelativistic shocks: theory and simulations, *MNRAS*, **328**, 393 (2001)
- [4] J. T. Frederiksen, C. B. Hededal, T. Haugbølle, and ÅNordlund, Collisionless Shocks - Magnetic Field Generation and Particle Acceleration, in Proc. From 1st NBSI on Beams and Jets in Gamma Ray Bursts, held at NBIfAFG/NORDITA, Copenhagen, Denmark, August, 1-6, 2002, (2003) (astro-ph/0303360)
- [5] K.-I. Nishikawa, P. Hardee, G. Richardson, R. Preece, H. Sol, and G. J. Fishman, Particle acceleration in relativistic jets due to Weibel instability, *ApJ*, **595**, 555 (2003)
- [6] L. O. Silva, R. A. Fonseca, J. W. Tonge, J. M. Dawson, W. B. Mori, and M. V. Medvedev, Near-equipartition magnetic field generation and non thermal particle acceleration, *ApJ*, **596**, L121 (2003)
- [7] J. T. Frederiksen, C. B. Hededal, T. Haugbølle, and ÅNordlund, *ApJ*, **608**, L13 (2004)
- [8] K.-I. Nishikawa, P. Hardee, G. Richardson, R. Preece, H. Sol, and G. J. Fishman, Particle Acceleration and Magnetic Field Generation in Electron-Positron Relativistic Shocks, *ApJ*, **623**, April 10 (2005) (astro-ph/0409702)
- [9] C. B. Hededal, T. Haugbølle, J. T. Frederiksen, and ÅNordlund, Non-Fermi power law acceleration in astrophysical plasma shocks, *ApJ*, **617**, L107 (2004)
- [10] C. B. Hededal, and K.-I. Nishikawa, The influence of an ambient magnetic field on relativistic collisionless plasma shocks, *ApJ*, **623**, in April (2005) (astro-ph/0412317)
- [11] E. S. Weibel, Spontaneously growing transverse waves in a plasma due to an anisotropic velocity distribution, *Phys. Rev. Lett.*, **2**, 83 (1959)
- [12] M. V. Medvedev, and A. Loeb, Generation of magnetic fields in the relativistic shock of gamma-ray burst sources, *ApJ*, **526**, 697 (1999)
- [13] K.-I. Nishikawa, P. Hardee, C. B. Hededal, G. Richardson, R. Preece, H. Sol, and G. J. Fishman, Relativistic Shocks: Particle Acceleration, Magnetic Field Generation, and Emission, in Proceeding of International Symposium on High Energy Gamma-Ray Astronomy, eds. F. A. Aharonian, H. J. Völk, & D. Horns, AIP Conf. Proc., v. 745, p. 534 (2005) (astro-ph/0410193)
- [14] K.-I. Nishikawa, P. Hardee, C. B. Hededal, G. Richardson, R. Preece, H. Sol, and G. J. Fishman, Particle Acceleration, Magnetic Field Generation, and Emission in Relativistic Shock. Advances in Space Research (35th COSPAR Scientific Assembly, Paris, 18-25 July 2004), in press, (2004) (astro-ph/04102660)
- [15] M. V. Medvedev, Theory of “Jitter” Radiation from Small-Scale Random Magnetic Fields and Prompt Emission from Gamma-Ray Burst Shocks, *ApJ*, **540**, 704 (2000)
- [16] G. D. Fleishman, Diffusive Synchrotron Radiation from Relativistic Shocks of Gamma-Ray Burst Sources, *ApJ*, submitted, (2005) (astro-ph/0502245)
- [17] M. V. Medvedev, Comment on the paper “Diffusive Synchrotron Radiation from Relativistic Shocks of Gamma-Ray Burst Sources” by G. D. Fleishman, *ApJ*, submitted, (2005) (astro-ph/0503463)
- [18] K.-I. Nishikawa, P. Hardee, C. B. Hededal, G. Richardson, H. Sol, R. Preece, and G. J. Fishman, Field Generation, and Emission in Relativistic Pair Jets, in 4th Workshop Gamma-Ray Bursts in the Afterglow Era, in press, (2005)